Mater.Phys.Mech.2 (2000) 63-69

COPPER-MATRIX Cu-HfO_2 NANOCOMPOSITE COMPACTS OF FULL DENSITY

K.Tousimi[1], R. Valiev[2] and A.R.Yavari[1]

[1] Euronano, LTPCM-CNRS, Institut National Polytechnique de Grenoble, B.P.75, 38402 St.Martin-d'Hères Campus, France
[2] Institute of Physics for Advanced Materials, Ufa State Aviation Technical University, Ufa 450000, Russia

Received: November 23, 2000

Abstract. Cu/HfO_2 nanocomposite powders were prepared by reactive milling under partial oxygen pressure as previously used to prepare Cu/ZrO_2 nanocomposites. Cu/HfO_2 nanocomposite powders with the same volumetric ceramic content were also prepared by direct milling of pure Cu with preformed HfO_2 powder. Interestingly, in the case of preparation by treactive milling, the resulting HfO_2 nanoparticles are amorphous. Direct milling of Cu and HfO_2 powder did not result in any amorphisation of the latter. Full density compacts of the nanocomposite powders were prepared by hot uniaxial pressing under vacuum and by torsion straining at room temperature under a load of 5 GPa. The microhardness of the resulting compacts are reported.

1. INTRODUCTION

Copper-ceramic nanocomposites such as Cu/HfO_2 and Cu/ZrO_2 can be prepared by reactive milling of the CuHf or CuZr alloys under partial pressure of oxygen [1-3]. If a partial pressure of O_2 in argon gas is introduced that just corresponds to the number of oxygen atoms needed to oxidise the metal in the mill, a gradual oxidation occurs that yields a nanograined oxide powder dispersion within a reduced, pure copper matrix. The reactions can be expressed as:

$$Cu_{1-x}A_x + x\,O_2 \rightarrow (1-x)\,Cu(nano) + x\,AO_2(nano) \qquad (1)$$

which occurs when the following three criteria are satisfied:

1) the formation enthalpy of the oxide AO_2 is strongly more negative than that of the alloy or $\Delta H(AO_2) << \Delta H(Cu_{1-x}A_x)$;
2) the formation enthalpy of the oxide AO_2 is strongly more negative than that of Cu_2O or $\Delta H(AO_2) << \Delta H(Cu_2O)$;
3) the amount (partial pressure) of O_2 introduced into the milling device corresponds exactly to that required for total oxidation of the A component and not more as per Eq.(1).

The volume fraction of the oxide nanodispersion is then determined by the initial fraction *x* of component A in the $Cu_{1-x}A_x$ alloy.

Of course nanocomposites of this type may also be obtainable by milling a mixture of Cu and the corresponding AO_2 oxide under inert gas atmospheres but as we will show, oxide nanoparticles obtained via reaction (1) are amorphous.

2. EXPERIMENTAL PROCEDURE

$Cu_{94.3}Hf_{5.7}$ alloys was prepared by induction heating then cast into thick foils then cut into small pieces before milling. The milling was performed in a vibrating mill containing a single 6 cm diameter steel ball evacuated and refilled with mixtures of Ar/O_2 gas with the total O_2 content fixed using Eq. (1) and the vial volume and the powder mass as described in [4]. The powders were of the order of 1 to 2 grams and after the required O_2 content was introduced, argon gas was added to take the total pressure in the vial above 1 atmosphere, using about 1.3 bars then sealed. A pressure gauge monitors the pressure inside each vial during the milling. Cu/HfO_2 nanocomposite powder was obtained according to Eq. (1) with a ceramic volume fraction of about 15%. Another nanocomposite powder of the same

Corresponding author: A.R. Yavari, e-mail : euronano@ltpcm.inpg.fr

© 2000 Advanced Study Center Co. Ltd.

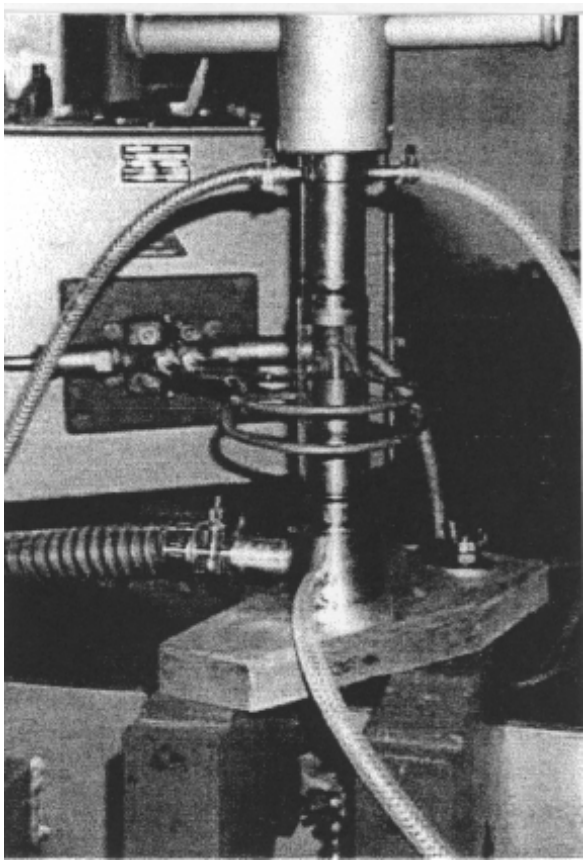

Fig. 1. A view of high pressure torsion equipment.

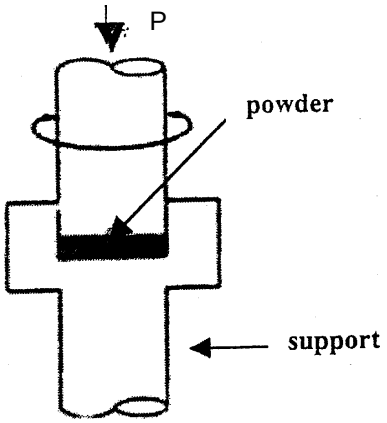

Fig. 2. Schematic representation of torsion straining at room temperature.

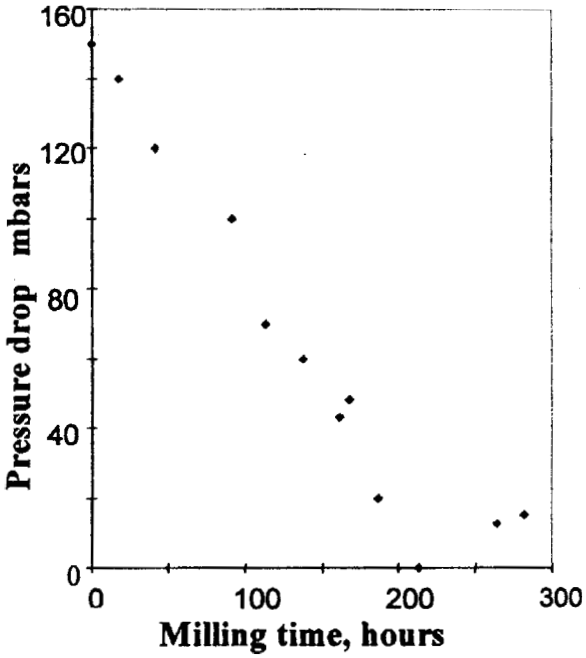

Fig. 3. O_2 partial pressure variation in the milling device during reactive milling of a $Cu_{80}Hf_{20}$ alloy.

composition was prepared by the direct milling of pure copper and preformed HfO_2 powder mixture. Compacts were then obtained by hot pressing the powder under vacuum where a thermocouple is placed below the powder chamber and by torsion straining at room temperature [5] as schematically represented in Fig. 1 and on the picture shown in Fig. 2. Microhardness values were obtained from the averaged results of indentations with a load of 200 g applied over 20 s. H_v was calculated as 1854 $F/d2$ where F is the load and d the mean value for the two diagonals of the pyramid imprint.

3. RESULTS AND DISCUSSION

Before examining the reactive milling of the $Cu_{94.3}Hf_{5,7}$ alloy and in order to establish the particularities of the oxide dispersion generated by the reaction with the oxygen partial pressure, we first examine the evolution of $Cu_{80}Hf_{20}$ where the pressure variations and the x-ray signal from the oxide phase are stronger due to the higher Hf content. Fig. 3 shows the O_2 partial pressure variation in the milling device during reactive milling of a $Cu_{80}Hf_{20}$ alloy. The pressure drop which occurs gradually over long milling times, corresponds to the total absorption of the O_2 molecules introduced in amounts given by Eq. (1) and the powder mass introduced into the milling device. This seems to imply that the Hf content of has been transformed totally to HfO_2 and the Cu in the matrix has been reduced to pure Cu. Fig. 4 shows the x-ray diffraction pattern of the $Cu_{80}Hf_{20}$ alloy after reactive milling.

The pattern does not show any Bragg peaks of crystalline HfO_2 phases but the Cu Bragg peaks here

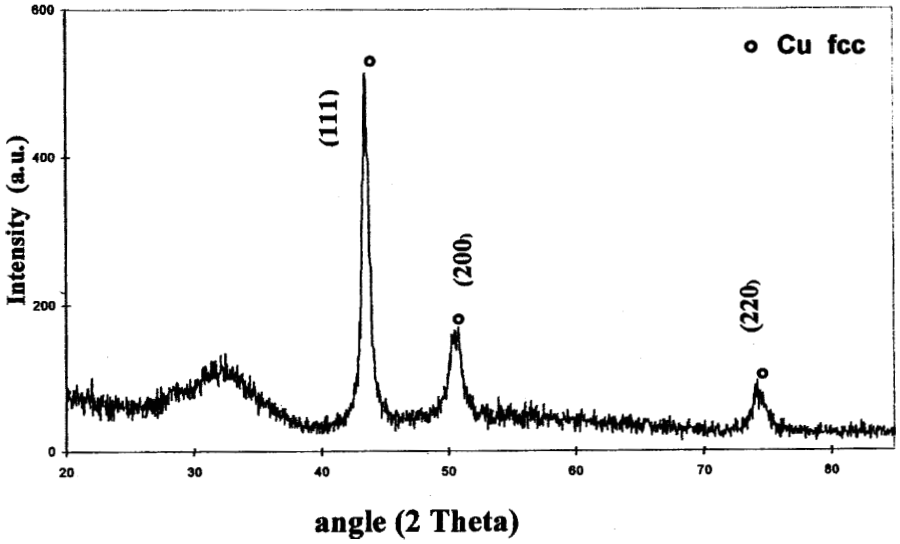

Fig. 4. X-ray diffraction pattern of the $Cu_{80}Hf_{20}$ alloy after reactive milling.

are broadened as expected after sever plastic deformation and grain refinement. In addition to broadened Cu Bragg peaks, a broad diffraction halo appears at low angles centred around 33 degrees.

Peak broadening analysis using the simple Scherrer method [6,7] on the Cu(111) peak, the de Keijser *et al* single peak analysis [8] that separates strain and crystal size contributions to the (111) peak broadening, and the multiple-peak Williamson and Hall analysis [9] were all applied for determination of the Cu coherent domain size [2] but the simpler Scherrer method was found to yield values as consistent with TEM images as the other methods. As given in Table I the grain size in the reactively milled powder is 15 nm with a precision within 4 nm.

Fig. 5 shows a calorimetric (DSC) thermogramme of the reacted powder and here we see a typical exothermic peak like in crystallisation of glasses occurring in the temperature range just above 400 °C. Fig. 6 shows the diffraction pattern of the reacted $Cu_{80}Hf_{20}$ after heat treatment at 500 °C. The amorphous halo has disappeared and the pattern now shows strong HfO_2 Bragg peaks. These results lead to the clear conclusion that the nanodispersed HfO_2 oxide product of reaction (1) is amorphous and crystallises above 400 °C.

Long-time milling of preformed crystalline HfO_2 and Cu powder under inert gas does not lead to the formation of amorphous HfO_2 [1,2].

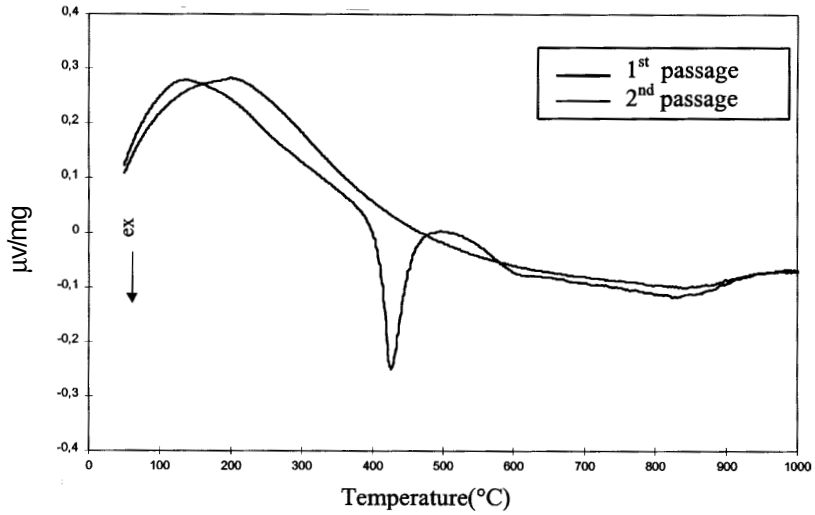

Fig. 5. Calorimetric (DSC) thermogramme of the reacted $Cu_{80}Hf_{20}$ powder with exothermic peak typical of crystallisation of glasses just above 400 °C.

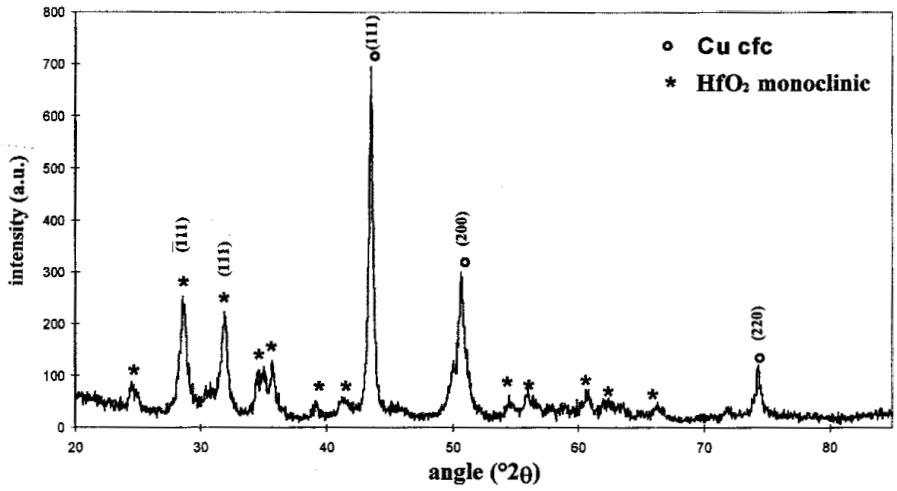

Fig. 6. X-ray diffraction pattern of reacted $Cu_{80}Hf_{20}$ after heat treatment at 500 °C. The amorphous halo has disappeared and the pattern now shows strong HfO_2 Bragg peaks.

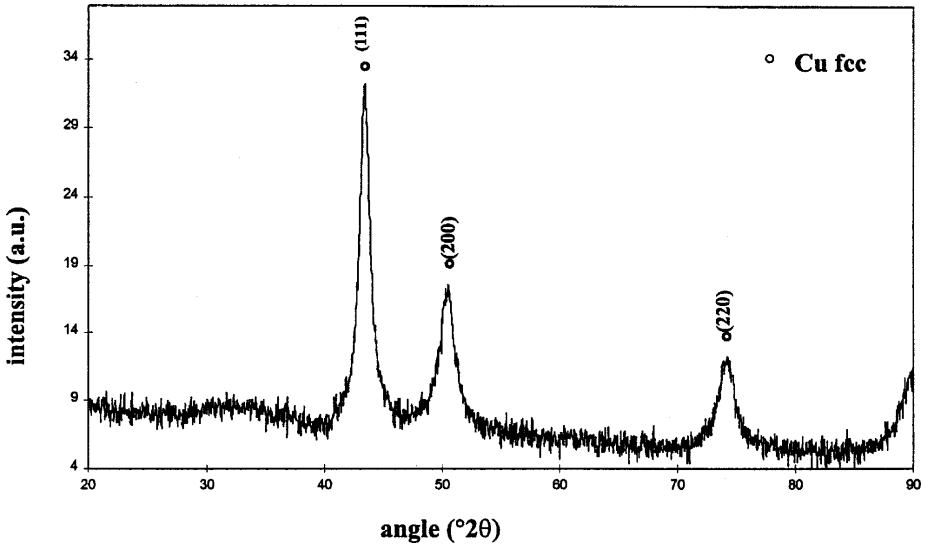

Fig. 7. X-ray diffraction pattern of $Cu_{94.3}Hf_{5,7}$ after reactive milling under oxygen partial pressure fixed by Eq. (1).

It is interesting to speculate on the process that leads to the formation of amorphous HfO_2 and ZrO_2 nanoparticles when reaction (1) occurs during milling. Many alloys transform to an amorphous structure after heavy deformation such as during milling (see for example the proceedings of the ISMANAM conference series published by Trans Tech). If so, as the $Cu_{1-x}A_x$ alloy undergoes multiple deformation and fracture cycles in the mill, the heavily deformed regions (around fracture surfaces and nanograin boundaries for example), may become amorphous.

Since these regions are those that are most exposed to the oxygen present in the vial, the oxide phase that forms there would be in an amorphous state also. In fact, $Cu_{80}Hf_{20}$ milled under argon gas (zero O_2 partial pressure) is fully amorphised by heavy deformation [2,3] and supports the idea that the amorphous nature of the HfO_2 nanoparticles of reaction (1) is likely to be because oxidation is preceded by amorphisation.

Next the alloy $Cu_{94.3}Hf_{5,7}$ was prepared in order to generate 15 volume % of HfO_2 after reactive milling. Fig. 7 shows the diffraction pattern of this alloy after reactive milling under oxygen partial pressure fixed by Eq. (1).

As in the diffraction pattern of Fig. 4 for $Cu_{80}Hf_{20}O_{40}$, Fig. 7 for the composition corresponding to $Cu_{94.3}Hf_{5,7}O_{11.4}$ also shows the broad halo of amorphous HfO_2 near 32 degrees but the signal is weaker due to a much lower volume fraction. This

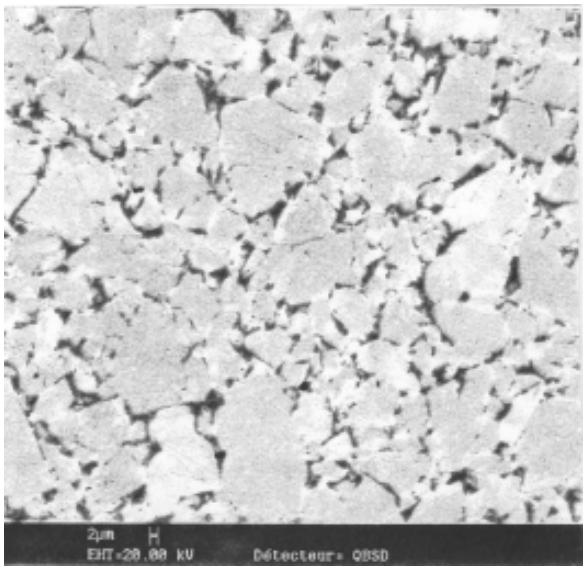

Fig. 8. Back-scattered electron SEM image of agglomerates in reacted $Cu_{94.3}Hf_{5.7}$ powder after hot pressing. The small white scale bar is 2 μm long.

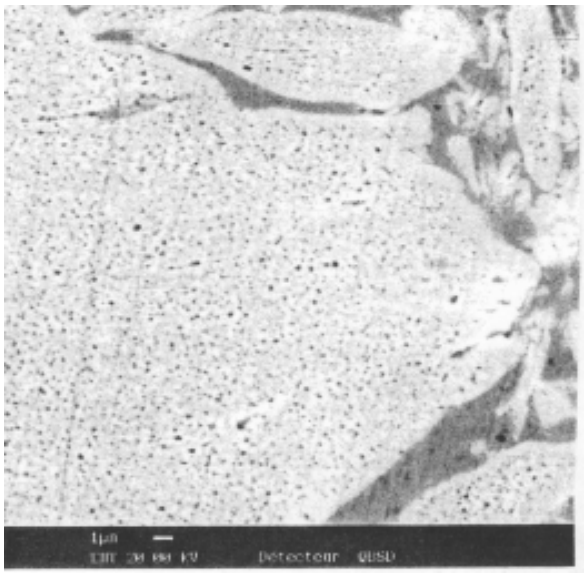

Fig. 9. Higher magnification SEM image of the compact of Fig. 8 showing agglomerates and interparticulate copper. The small white scale bar is 1 μm long.

powder was then hot pressed to form compacts. Fig. 8 shows a back-scattered electron SEM image of the powder after hot pressing. The clear, rock-like regions correspond to the morphology of agglomerates in the reactively milled powder.

The dark inter-agglomerate regions are pure copper that has oozed out of the agglomerates during hot pressing. The agglomerates have thus become Cu-poor and there are two types of copper regions, the micron-scale inter- agglomerate copper and the nanometric copper within the agglomerates as seen in the higher magnification SEM image of Fig. 9. TEM electron diffraction patterns taken from the inter-agglomerate regions and the agglomerates themselves as presented in Fig. 10 clearly show that the inter- agglomerate copper is fairly coarse grained while the diffraction rings from the Cu within the agglomerates are rings of small spots corresponding to nanoparticulate copper.

Similar compacts were prepared in disks of about 300 mkm thickness and 1 cm diameter by torsion straining under uniaxial pressure of 5 GPa. The rotation speed of the load axis perpendicular to the compact plane was about 2 to 3 revolutions per minute.

Fig. 11 shows a back scattered electron SEM image of a compact of the same Cu/HfO_2 nanocomposite powder used for the hot pressed sample of Fig. 8 here prepared by torsion straining at room temperature.

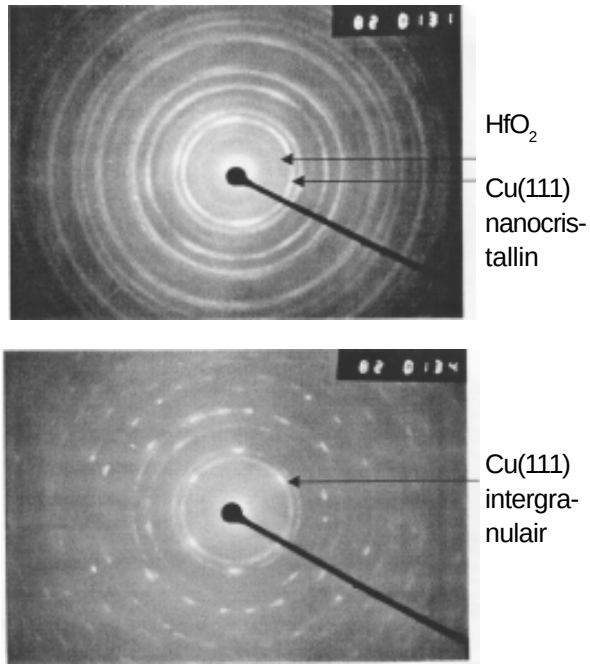

Fig. 10. TEM electron diffraction patterns from the inter-agglomerate regions (bottom) and the agglomerates themselves (top).

It is seen that while the compact structure is fully dense and highly strained as evidenced by intensely sheared regions, the initial agglomerates obtained by milling are no longer visible and no significant inter-agglomerate copper has oozed out as

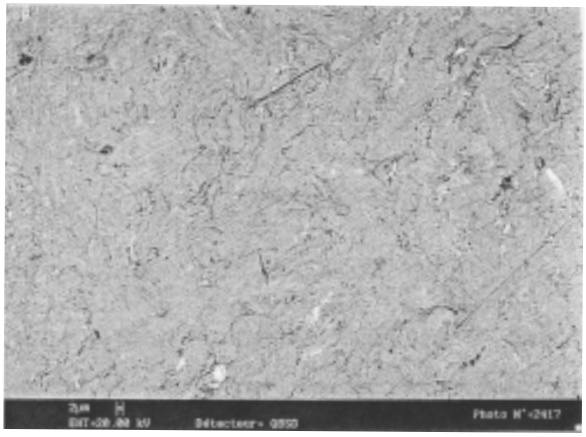

Fig. 11. Back scattered electron SEM image of a compact of the Cu/HfO_2 powder here prepared by torsion straining at room temperature.

in Fig. 8's black region. Since the straining is performed at room temperatures, inspite of some heating due to deformation work, the compact remains far below the crystallisation temperature of the amorphous HfO_2 particles and therefore represent a unique bulk sample of copper with a nanodispersion of amorphous HfO_2 particles.

Table 1 summarizes the average Cu grain size values before and after hot-pressing or torsion straining. In the hot pressed sample it is to be noted that D = 40 nm is a value obtained from the convoluted x-ray intensity from both nano-Cu in the agglomerates and micro-Cu in the interparticulte regions seen for example in Fig. 9.

The Cu that remains within the agglomerates is expected to have a significantly lower grain size. In the case of the torsion strained sample the grain size does not grow. The apparent increase in D is due to the development of texture that has not been accounted for in the Scherrer derivation.

Table 2 shows the hardness of the various Cu-15 vol.% HfO_2 nanocomposites, prepared by reactive milling or milling of Cu and HfO_2 powders under inert gas then compacted to full density by hot pressing at the given temperatures or by torsion straining at room temperature. The hardnesses are much higher for the compacts of nanocomposites obtained by reactive milling as compared to compacts of Cu milled with preformed HfO_2 powder when hot pressed at the same temperature and pressure even though the pressing temperature is higher than the crystallisation temperature of the amorphous HfO_2 dispersion in the former. The much higher mechanical resistance of compacts containing HfO_2 particles formed during reactive milling must therefore be attributed to a finer and more homogeneous distribution in the copper matrix.

The yield strength also increases with decreasing temperature of hot pressing as at lower temperatures less of the copper in the agglomerates oozes out to the inter-agglomerate boundaries (see Fig. 8 and 9). Finally, the very high values of yield strength and hardness close to 4 GPa is obtained in torsion strained compacts of the Cu-HfO_2 nanocomposites obtained by reactive milling (Eq.(1)). This is expected because as seen in Fig.11, none of the Cu oozes out to form coarse grain inter-agglomerate layers as in the hot pressed samples. All the Cu content therefore remains nanocrystalline and contributes to the increased hardening by the Hall-Petch effect.

4. CONCLUSIONS

Reactive milling of $Cu_{80}Hf_{20}$ under partial O_2 pressure as determined by Eq.(1) leads to the formation of stoichiometric or near stoichiometric distribution HfO_2 amorphous particles within a purified Cu matrix as detected by x-ray and electron diffraction. The DSC thermograms indicate that the amorphous phase crystallises above 400 °C and annealing leads to the appearance of HfO_2 Bragg peaks and the disappearance of the amorphous halo in x-ray diffraction patterns as expected. The formation of these amorphous oxides which does not occur even after long milling of preformed crystalline oxide powders with Cu is consistent with the formation of the oxides being preceded by amorphisation of the severely deformed regions of the alloy powders. Full density compacts of Cu-15 vol.% HfO_2 were prepared both by hot uniaxial pressing and by torsion straining at room temperature. It was found that the compacts' mechanical resistance increases with decreasing temperature of compaction. Microscopic examination of the compacts revealed that hot press-

Table I. The average Cu grain size values before and after hot-pressing or torsion straining.

Cu crystal size (nm)	(reactively milled) Cu/HfO_2	(hot pressed 450 °C) Cu/HfO_2	(torsion strained) Cu/HfO_2
$D_{Scherrer\ (111)}$	15	40	18

Table 2.

	Preformed Cu/HfO_2 Hot Pressed 650 °C	Reactively milled Cu/HfO_2 Hot Pressed 650 °C	Reactively milled Cu/HfO_2 Hot Pressed 450 °C	Preformed Cu/HfO_2 torsion strained	Reactively milled Cu/HfO_2 torsion strained
Hardness GPa	1.34	2.55	2.74	3.57	3.80

ing leads to part of the Cu nanomixed with $Cu_{80}Hf_{20}$ oozing out of the agglomerates. The ejected Cu then forms coarse grained interparticulate regions and leads to softening. This phenomenon does not occur in compacts obtained by torsion straining which maintain hardnesses up to 3.8 GPa.

ACKNOWLEDGEMENTS

This work was funded in part by INTAS project 99-1741.

REFERENCES

[1] K. Tousimi and A.R.Yavari // *J. Metastable & Nanocrystalline Mater.* **7** (2000) 7.
[2] K. Tousimi, *Ph.D. Thesis* (Institut National Polytechnique de Grenoble, Nov. 1999).
[3] K. Tousimi and A.R. Yavari // *International J. Non-Equilibrium Processing,* in press.
[4] K K.Tousimi, W.J. Botta F.W.J. and A.R. Yavari // *Mater. Sci. Forum* **312** (1999) 73.
[5] R. Valiev // *Mater. Sci. Eng.* **A234-236** (1997) 59.
[6] H. Klug and L. Alexander*, X-Ray Diffraction Procedures for Polycrustalline and Amorphous Materials,* (Wiley, 1955).
[7] P.Scherrer // *Göttinger Nachrichten* **2** (1918) 98.
[8] Th.H.De Keijser, J.I.Langford, E.J.Mittemeijer and B.P.Vogels // *J.Appl.Cryst.* **15** (1982) 308.
[9] G.K.Williamson and W.H.Hall // *Acta Metall.* **1** (1953) 22.